REPORT R-1033 MARCH 1985 UILU-ENG 85-2208

CSL COORDINATED SCIENCE LABORATORY

A STUDY OF CROSSTALK AND DISTORTION OF HIGH SPEED PULSES IN DIGITAL CIRCUITS

S. CASTILLO
R. MITTRA

UNIVERSITY OF ILLINOIS – URBANA, ILLINOIS

Unclassified

SECURITY CLASSIFICATION OF THIS PAGE

REPORT DOCUMENTATION PAGE

1a. REPORT SECURITY CLASSIFICATION Unclassified	1b. RESTRICTIVE MARKINGS None
2a. SECURITY CLASSIFICATION AUTHORITY N/A	3. DISTRIBUTION/AVAILABILITY OF REPORT Approved for public release, distribution unlimited.
2b. DECLASSIFICATION/DOWNGRADING SCHEDULE N/A	
4. PERFORMING ORGANIZATION REPORT NUMBER(S) R-report #1033	5. MONITORING ORGANIZATION REPORT NUMBER(S) N/A
6a. NAME OF PERFORMING ORGANIZATION Coordinated Science Lab. Univ. of Illinois 6b. OFFICE SYMBOL (If applicable) N/A	7a. NAME OF MONITORING ORGANIZATION Office of Naval Research
6c. ADDRESS (City, State and ZIP Code) 1101 W. Springfield Avenue Urbana, Illinois 61801	7b. ADDRESS (City, State and ZIP Code) 800 N. Quincy Street Arlington, VA 22217
8a. NAME OF FUNDING/SPONSORING ORGANIZATION 8b. OFFICE SYMBOL (If applicable) N/A	9. PROCUREMENT INSTRUMENT IDENTIFICATION NUMBER Contract #N00014-84-C-0149
8c. ADDRESS (City, State and ZIP Code)	10. SOURCE OF FUNDING NOS. PROGRAM ELEMENT NO. / PROJECT NO. / TASK NO. / WORK UNIT NO.
11. TITLE (Include Security Classification) A Study of Crosstalk & Distortion of High Speed Pulse in Digital Circuits	
12. PERSONAL AUTHOR(S) S. Castillo and R. Mittra	
13a. TYPE OF REPORT Technical 13b. TIME COVERED FROM _____ TO _____	14. DATE OF REPORT (Yr., Mo., Day) March 1985 15. PAGE COUNT 55
16. SUPPLEMENTARY NOTATION N/A	
17. COSATI CODES FIELD / GROUP / SUB. GR.	18. SUBJECT TERMS (Continue on reverse if necessary and identify by block number) pulse propagation; crosstalk noise; micro electronic packaging; multiconductor transmission lines.

19. ABSTRACT (Continue on reverse if necessary and identify by block number)

In this report crosstalk and distortion of high speed pulses due to multiple reflections are studied. The moment method is used to solve for the currents and charges on a set of parallel microstrip transmission lines. Next, these solutions are employed to construct the capacitance and inductance matrices for the system. A modal analysis of an n-line transmission line system is used to evaluate the dependence of crosstalk on line spacing and input pulse risetime. Other results are given which demonstrate the difficulty of obtaining accurate data for poorly matched loads.

20. DISTRIBUTION/AVAILABILITY OF ABSTRACT UNCLASSIFIED/UNLIMITED ☒ SAME AS RPT. ☐ DTIC USERS ☐	21. ABSTRACT SECURITY CLASSIFICATION Unclassified
22a. NAME OF RESPONSIBLE INDIVIDUAL	22b. TELEPHONE NUMBER (Include Area Code) 22c. OFFICE SYMBOL None

DD FORM 1473, 83 APR EDITION OF 1 JAN 73 IS OBSOLETE.

Unclassified

SECURITY CLASSIFICATION OF THIS PAGE

A STUDY OF CROSSTALK AND DISTORTION OF HIGH SPEED PULSES IN DIGITAL CIRCUITS

S. Castillo and R. Mittra

Department of Electricl & Computer Engineering
University of Illinois
Urbana, Illinois

The work reported in this paper was supported in part by the Joint Services Electronics Program, N00014-84-C-0149.

ABSTRACT

In this report crosstalk and distortion of high speed pulses due to multiple reflections are studied. The moment method is used to solve for the currents and charges on a set of parallel microstrip transmission lines. Next, these solutions are employed to construct the capacitance and inductance matrices for the system. A modal analysis of an n-line transmission line system is used to evaluate the dependence of crosstalk on line spacing and input pulse risetime. Other results are given which demonstrate the difficulty of obtaining accurate data for poorly matched loads.

TABLE OF CONTENTS

1. INTRODUCTION

This report is an analysis of crosstalk and reflections in digital circuits on printed circuit (pc) boards. Every year packaging densities go up and switching times come down with the result being an increase in crosstalk and reflections in the circuits. Therefore, a need has risen for applying microwave techniques to digital circuits in order to be able to predict crosstalk and reflection voltages in a given circuit which may result in false switching of the devices.

We begin in chapter two by analyzing a simple transmission line system consisting of two parallel microstrip transmission lines that are infinite in length. The network analysis of electromagnetic fields is used to derive a superposition integral relating the charge distribution on a strip to the voltage on the strip. This is done by finding a Green's function due to an arbitrary current source placed at the z=0 plane (fig. 1) (page 5) in a transmission line set up in the transverse direction. Galerkin's method is used to find an approximate solution for the charge distribution. The application of Galerkin's method resulted in several integrals that could only be done numerically. These integrals were found to have slow convergence when calculated on a large Cyber computer system. Asymptotic approximations -- applied to the integrals along with a good choice of basis functions resulted in fast convergence. From the calculated charge distribution the capacitance coefficients are then solved for.

The same analysis is then used to derive a superposition integral relating the current distribution on a strip to the flux linking the strip to the ground plane. Again, Galerkin's method was applied to give an approximate solution for the current distribution on the strip. The inductance coefficients are then solved for from the calculated current distribution.

In chapter three a general analysis of an N-conductor transmission line system is presented. The technique used is one of modal analysis.

The telegrapher equations for a multi-conductor transmission line system are combined to give an eigenvalue equation. The eigenvalues are the inverse of the propagation constants of the system squared and are found from the product of the inductance and capacitance matrices associated with the system. The eigenvectors represent the modal voltage amplitudes. The idea of modal transmission and reflection matrices is developed here.

The general modal transmission line theory is then specialized to the original problem of two parallel microstrip transmission lines terminated by digital devices. The inductance and capacitance matrices are found through the techniques presented in chapter two.

A computer program was written from the results of the analysis given in chapters two and three. The program assumes the input to the system to be a pulse with rise time and length specified by the user. The program uses a time

stepping technique where the input voltage ramp of the pulse is approximated by a series of step functions.

Numerical results are given for the load voltages in the system as a function of time. Different sets of results are presented for varying rise times of the input pulse as well as varying dimensions of the microstrip transmission lines.

2. DETERMINATION OF CAPACITANCE AND INDUCTANCE COEFFICIENT MATRICES

In this chapter, the inductance and capacitance coefficient matrices associated with a system of two parallel microstrip transmission lines that are infinite in length are found. From elementary electrostatics we have

$$[Q] = [C][V] \tag{2-1a}$$

$$[\phi] = [L][I] \tag{2-1b}$$

The problem can be solved by the formulation of two integral equations. One integral equation relates the voltage on the strip to the charge distribution on the strip, and the other relates the current distribution on the strip to the flux linking the strip to the reference conductor ground plane. The results from these integral equations are then used in equations (2-1) to solve for both the capacitance and inductance matrices.

2.1 Formulation of the Integral Relating Voltage and Charge.

Figure 1 shows the geometry of the initial problem. The conductor is assumed to be perfectly conducting with zero thickness and infinite length. The ground planes and dielectric are assumed to extend to infinity in all directions with the dielectric being lossless. This is a good assumption for the strip width being much less than that of the width of the ground planes and dielectric.

The transverse fields in each region are given by the following integral [1], [8].

$$\begin{matrix}\bar{E}_t^{(i)} \\ \bar{H}_t^{(i)}\end{matrix} = \sum_{\ell=1}^{2} \left\{ \int_{-\infty}^{\infty} \begin{matrix}\bar{V}_\ell^{(i)}(\alpha;z)\,\bar{f}_\ell(\alpha;x) \\ I_\ell^{(i)}(\alpha;z)\,x\bar{f}_\ell(\alpha;x)\end{matrix} \right\} d\alpha e^{-j\beta_o y} \qquad (2\text{-}2)$$

$$i=1,2$$

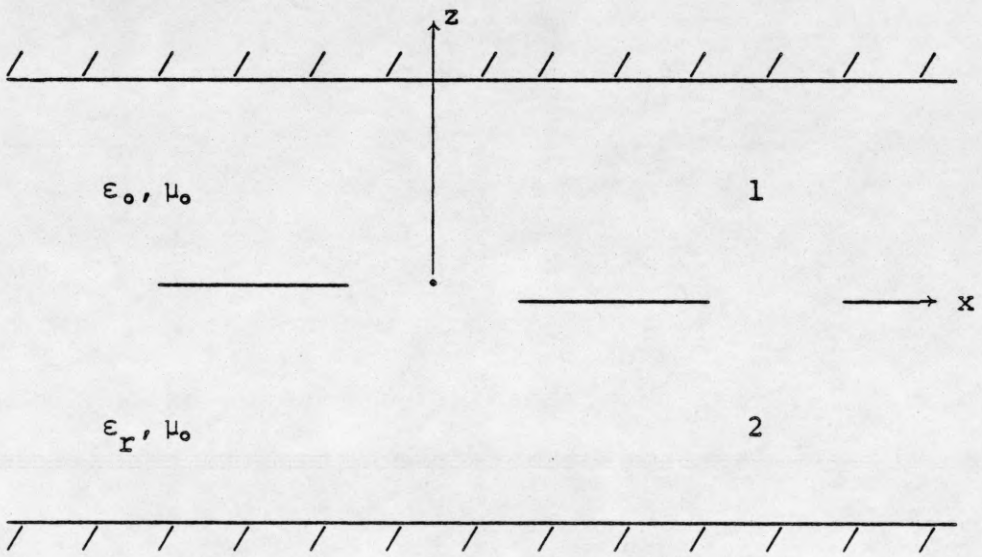

Figure 1 - Microstrip Cross Section

where

$$\bar{f}_1 = \frac{j}{\sqrt{2\pi}} \bar{K}_o e^{-j\alpha x} \quad , \quad \bar{f}_2 = \bar{f}_1 \times \hat{z}_o$$

$$\bar{K}_o = \frac{\bar{K}}{K}$$

$$\bar{K} = \hat{x}_o \alpha + \hat{y}_o \beta_o, \quad K = |\bar{K}|$$

β_o is the propagation constant in the y-direction, $\hat{x}_o$, $\hat{y}_o$, and $\hat{z}_o$ are the x, y, and z directed unit vectors respectively, and $\ell=1$ and $\ell=2$ represent TM waves ($H_z=0$) and TE waves ($E_z=0$) respectively.

By substituting equation (2-2) into Maxwell's curl equations we can get the following expression

$$-\frac{d}{dz}V_\ell^{(i)} = jk_\ell^{(i)} Z_\ell^{(i)} I_\ell^{(i)}$$

$$-\frac{d}{dz}I_\ell^{(i)} = jk_\ell^{(i)} Y_\ell^{(i)} V_\ell^{(i)} \qquad (2\text{-}3)$$

where

$$k_\ell^{(i)} = \sqrt{K^{2(i)} - K^2} \qquad j = \sqrt{-1}$$

$$Z_\ell\Big/_{\ell=1}^{(i)} = \frac{k_1^{(i)}}{w\,\varepsilon_i} \qquad Z_\ell\Big/_{\ell=2}^{(i)} = \frac{\omega\,\mu_o}{k_2^{(i)}}$$

$$Y_\ell^{(i)} = \frac{1}{Z_\ell^{(i)}} \qquad K^{2(i)} = \omega^2 \varepsilon^{(i)} \mu_o$$

Equations (2-3) are the transmission line equations in each region. $k_\ell^{(i)}$ is the propagation constant in the z direction for both the TE and TM waves for each media and $Z_\ell^{(i)}$ is the impedance in the z-direction for both the TE and TM waves in each media.

Figure 2 shows a transmission line in a transverse section of the microstrip line. The shorts at z=d and z=-t correspond to the ground planes located at those points. The boundary conditions to be satisfied are as follows:

$$V_\ell^{(1)}(d) = 0 \qquad (2\text{-}4a)$$

$$V_\ell^{(1)}(0^+) = V_\ell^{(2)}(0^-) \qquad (2\text{-}4b)$$

$$I_\ell^{(1)}(0^+) - I_\ell^{(2)}(0^-) = i_\ell \qquad (2\text{-}4c)$$

$$V_\ell^{(2)}(-t) = 0 \qquad (2\text{-}4d)$$

Boundary conditions (2-4a) and (2-4d) state that the voltages

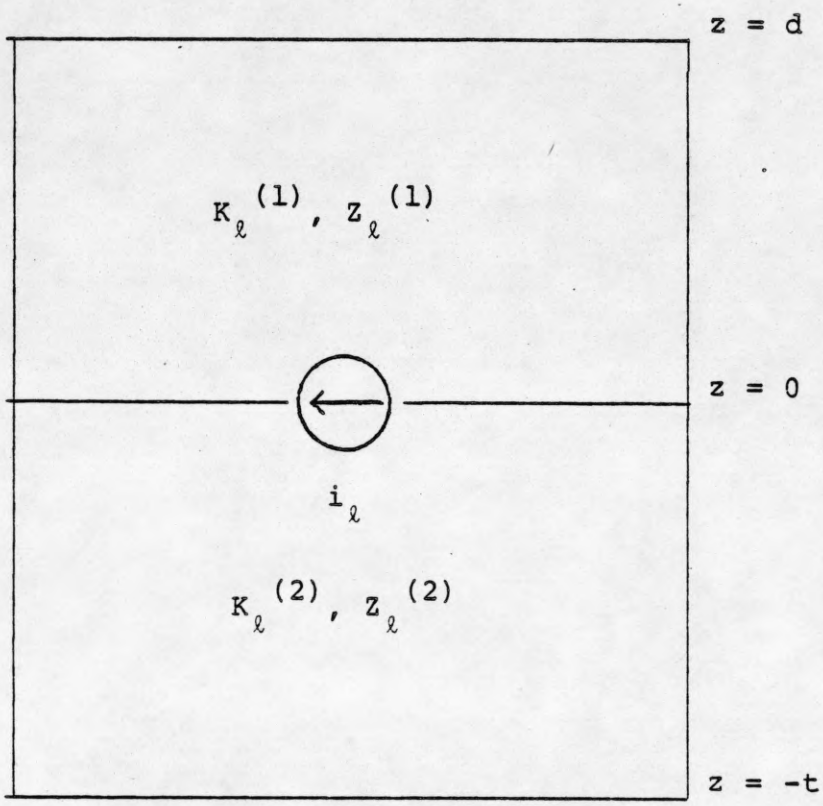

Figure 2 - Equivalent Transmission Line Circuit for Transverse Section of Microstrip

on the ground planes are zero. Boundary condition (2-4b) states that the voltage is continuous across the z=0 plane and boundary condition (2-4c) states that the currents in each region are discontinuous by the test current, i_ℓ.

The voltage and current in region 1 are given by

$$V_\ell^{(1)}(z) = Ae^{-jk_\ell^{(1)}z} + Be^{jk_\ell^{(1)}z} \tag{2-5}$$

$$I_\ell^{(1)}(z) = \frac{1}{Z_\ell^{(1)}}\left[Ae^{-jk_\ell^{(1)}z} - Be^{jk_\ell^{(1)}z}\right]. \tag{2-6}$$

The voltage and current in region 2 are given by

$$V_\ell^{(2)}(z) = Ce^{-jk_\ell^{(2)}z} + De^{jk_\ell^{(2)}z} \tag{2-7}$$

$$I_\ell^{(2)}(z) = \frac{1}{Z_\ell^{(1)}}\left[Ce^{-jk_\ell^{(2)}z} - De^{jk_\ell^{(2)}z}\right] \tag{2-8}$$

A negative sign in the exponent indicates a wave traveling in the positive z direction.

By applying the boundary conditions (2-4a), (2-4b), (2-4c), and (2-4d) to equations (2-5) through (2-8) we have the following

$$Ae^{-jk_\ell^{(1)}d} + Be^{jk_\ell^{(1)}d} = 0,$$

$$A + B = C + D,$$

$$\frac{1}{Z_\ell^{(1)}}[A - B] - \frac{1}{Z_\ell^{(2)}}[C - D] = i_\ell,$$

$$Ce^{ik_\ell^{(2)}t} + De^{-jk_\ell^{(2)}t} = 0.$$

More conveniently we can write,

$$\begin{bmatrix} e^{-jk_\ell^{(1)}d} & e^{jk_\ell^{(1)}d} & 0 & 0 \\ 1 & 1 & -1 & -1 \\ \frac{1}{Z_\ell^{(1)}} & -\frac{1}{Z_\ell^{(1)}} & -\frac{1}{Z_\ell^{(2)}} & \frac{1}{Z_\ell^{(2)}} \\ 0 & 0 & e^{jk_\ell^{(2)}t} & e^{-jk_\ell^{(2)}t} \end{bmatrix} \begin{bmatrix} A \\ B \\ C \\ D \end{bmatrix} = \begin{bmatrix} 0 \\ 0 \\ i_\ell \\ 0 \end{bmatrix} \quad (2\text{-}9)$$

From the matrix equation (2-9) the constants A, B, C, and D are easily solved for and are given as

$$A = i_\ell e^{jk_\ell^{(1)}d} \sin(k_\ell^{(2)}t)\Delta' \quad (2\text{-}10)$$

$$B = -i_\ell e^{-jk_\ell^{(1)}d} \sin(k_\ell^{(2)}t)\Delta' \quad (2\text{-}11)$$

$$C = -i_\ell e^{-jk_\ell^{(2)}t} \sin(k_\ell^{(1)}d)\Delta' \quad (2\text{-}12)$$

$$D = i_\ell e^{jk_\ell^{(2)}t} \sin(k_\ell^{(1)}d)\Delta' \quad (2\text{-}13)$$

where

$$\Delta' = \frac{Z_\ell^{(1)}Z_\ell^{(2)}}{2[Z_\ell^{(1)}\cos(k_\ell^{(2)}t)\sin(k_\ell^{(1)}d)+Z_\ell^{(2)}\sin(k_\ell^{(2)}t)\cos(k_\ell^{(1)}d)]} .$$

Substituting (2-10) through (2-13) into equations (2-6) and (2-8) yields

$$I_\ell^{(1)} = \frac{2}{Z_\ell^{(1)}}\sin(k_\ell^{(2)}t)\Delta'\cos(k_\ell^{(1)}(d-z))\, i_\ell \quad (2\text{-}14)$$

$$I_\ell^{(2)} = -\frac{2}{Z_\ell^{(2)}}\sin(k_\ell^{(1)}d)\Delta'\cos(k_\ell^{(2)}(t+z))\, i_\ell . \quad (2\text{-}15)$$

The test current i_ℓ can be expressed by the following Fourier integral in the x direction

$$i_\ell = -\int_{-\infty}^{\infty} \bar{f}_\ell(\alpha,x') \cdot \bar{i}(x')dx' \qquad (2\text{-}16)$$

where $\bar{i}(x') = \hat{x}_o i_x(x) + \hat{y}_o i_y(x')$.

In digital circuits the bandwidth of the signal is determined by the rise time of the pulses being transmitted. For rise times on the order of one nsec., the -3 dB frequency is .35 GHz. Studies done by Kitazawa [1] indicate that a static approximation would be quite useful at frequencies this low on typical printed circuit boards. The static approximation simplifies the analysis a good deal.

Expanding the expression for the transverse H-field and applying the approximation $\beta_o \to 0$ we have

$$\bar{H}_t^{(i)} = \int_{-\infty}^{\infty} I_1^{(i)}(\alpha;z)\frac{\alpha\hat{y}_o}{|\alpha|}\frac{j}{\sqrt{2\pi}} e^{-j\alpha x}d\alpha \qquad (2\text{-}17)$$

$$+ \int_{-\infty}^{\infty} I_2^{(i)}(\alpha;z)\frac{\alpha\hat{x}_o}{|\alpha|}\frac{j}{\sqrt{2\pi}} e^{-j\alpha x}d\alpha$$

The voltage on the strip may be found by either integrating the E_z- field in region one from 0 to d or integrating the E_z-field in region two from -t to 0. The choice here is arbitrary so the succeeding equations will all apply to region one only. The E_z field component only can be found from the ℓ=1 TM field since no E_z component exists for the ℓ=2 TE field. Now,

$$\lim_{\beta_o \to o} I_1^{(1)}(\alpha;z) = \frac{\cosh[(z-d)]|\alpha|]\ \ i_1(\alpha)}{\{\varepsilon_r \coth(|\alpha|t)+\coth(|\alpha|\ d)\}\sinh(|\alpha|\ d)}$$

and

$$i_1(\alpha) = \int_{-\infty}^{\infty} \frac{j}{\sqrt{2\pi}} e^{j\alpha x'} i_x(x')dx'$$

Therefore, the transverse H field component of the TM wave is given by

$$H_{t_1}^{(1)} = \frac{-1}{2\pi} \int_{-\infty}^{\infty}\int_{-\infty}^{\infty} \frac{\cosh[(z-d)|\alpha|]}{\{\varepsilon_r \coth(|\alpha|t)+\coth(|\alpha|d)\}\sinh(|\alpha|d)}$$

$$i_x(x')e^{j\alpha(x' - x)}dx'd\alpha$$

The E_z component is found from the H field from Maxwell's curl equation which can be expressed as

$$Ez^{(1)} = \frac{1}{j\omega\varepsilon^{(1)}} \nabla \cdot (\bar{H}_{t_1}^{(1)} \times \hat{Z}_o) \qquad (2\text{-}18)$$

$$= \frac{1}{2\pi\omega\varepsilon^{(1)}} \int_{-\infty}^{\infty} \frac{\alpha\cosh[(z - d)|\alpha|]}{\{\varepsilon r\coth(|\alpha|t)+\coth(|\alpha|d)\}\sinh(|\alpha|d)} \cdot$$

$$i_x(x')e^{-j\alpha(x-x')}dx'd\alpha.$$

To get equation (2-18) into a form that relates the charge distribution to the electric field Ez, the integration with respect to x' is performed by parts and the equation of continuity

$$-j\omega\sigma(x') = \frac{d}{dx'} i_x(x') \qquad (2\text{-}19)$$

is used. Equation (2-18) then becomes

$$E_z^{(1)} = \frac{1}{2\pi\omega\varepsilon^{(1)}} \int_{-\infty}^{\infty} \{ \int \alpha T(\alpha;z) e^{-j\alpha(x-x')} dx' i_x(x') \Big|_{-\infty}^{\infty}$$

$$- \int_{-\infty}^{\infty} \left(\int \alpha T(\alpha;z) e^{-i\alpha(x-x')} dx' \right) \frac{di_x(x')}{dx'} dx' \} \, d\alpha \qquad (2\text{-}20)$$

where $T = \dfrac{\cosh[(z-d)|\alpha|]}{\{\varepsilon r \coth(|\alpha|t) + \coth(|\alpha|d)\sinh(|\alpha|d)}$.

The first term in equation (2-20) goes to zero since $i_x(\infty) = i_x(-\infty)$ so that equation (2-20) becomes

$$E_z^{(1)} = \frac{-1}{2\pi\omega\varepsilon^{(1)}} \int_{-\infty}^{\infty} \int_{-\infty}^{\infty} T_1(\alpha;z) e^{-j\alpha x} \frac{e^{j\alpha x'}}{j\alpha} \alpha(-j\omega\sigma(x')) dx' d\alpha$$

$$= \frac{1}{2\pi\varepsilon^{(1)}} \int_{-\infty}^{\infty} \int_{-\infty}^{\infty} T_1(\alpha;z) e^{j\alpha(x'-x)} \sigma(x') dx' d\alpha \qquad (2\text{-}21)$$

Now, the voltage on the strip conductor is just the integral of the z component of the electric field from the top ground plane to the strip.

$$V(x) = \int_0^d E_z(x,z) dz .$$

$$V(x) = \frac{1}{2\pi\varepsilon^{(1)}} \int_{-\infty}^{\infty} \int_{-\infty}^{\infty} \frac{6(x') \, e^{-j\alpha(x-x')}}{\{\varepsilon r \coth(|\alpha|t) + \coth(|\alpha|d)\}|\alpha|} d\alpha dx' \qquad (2\text{-}22)$$

The structure of the microstrip used in digital circuits such as printed circuit boards does not have the top ground plane shown in figure 1. It is easy to transform the original problem to that of the problem we are concerned with by taking the limit of V(x) as d goes to infinity. The only term involving the constant d is $\coth(|\alpha|d)$ which goes to one as d goes to infinity. Therefore, equation (2-22) becomes

$$V(x) = \int_{-\infty}^{\infty} \int G(\alpha, x|x') \sigma(x') d\alpha dx' \qquad (2\text{-}23)$$

where

$$G(\alpha, x|x') = \frac{1}{2\pi\varepsilon_o} \frac{e^{-j\alpha(x-x')}}{\varepsilon_r \coth(|\alpha|t)+1} \frac{1}{|\alpha|} \qquad (2\text{-}24)$$

All modes of propagation for the two strip case can be expressed as a linear combination of the basis modes called the even mode and the odd mode. The even mode is the mode for which the potential on the two strips is equal. The odd mode is the mode for which the potential on the two strips is equal in amplitude but opposite in sign. Therefore, symmetry can be used to simplify the expression for voltage. Equations (2-23) and (2-24) then become

$$V(x) = \int_{-\infty}^{\infty} G(\alpha, x|x')\sigma(x')\,d\alpha dx' \qquad (2\text{-}25)$$

where

$$G(\alpha, x|x') = \frac{2}{\pi\varepsilon_o} \frac{F(\alpha)}{\alpha} \cos\alpha x \cos\alpha x' \qquad (2\text{-}26)$$

for the even mode

$$= \frac{2}{\pi\varepsilon_o} \frac{F(\alpha)}{\alpha} \sin\alpha x \sin\alpha x'$$

for the odd mode

and

$$F(\alpha) = \frac{1}{\varepsilon_r \coth(\alpha t)+1}$$

Since charge will only exist on the conductor, then the integration with respect to x' is zero at all points on the plane not occupied by the conductor. Equation (2-25) then becomes

$$V(x) = \int_a^b \int_o^\infty G(\alpha, x|x') \sigma(x'|d\alpha dx' \qquad (2\text{-}27)$$

where G is as given before.

2.2 Solution of the Voltage Charge Integral Equation.

Prior to the advent of large computers, engineers and scientists would try to find some form of a given integral equation which could be solved analytically. Now, computers can be used to find highly accurate "approximate" solutions. The integral equation that was derived in the previous section relating voltage to charge would be very difficult if not impossible to solve. The method that is commonly used to solve these problems is called the method of moments.

It is assumed that the reader has some background in linear spaces. A more detailed explanation is given in reference [7]. Given,

$$L(\mu) = s$$

where s is known and μ is unknown, then μ may be found by

$$\mu = L^{-1}(s).$$

To do this, μ is expanded in a set of linearly independent basis functions

$$\mu = \sum_{n=1}^{N} a_n \mu_n.$$

Since any function may be exactly represented as an infinite series, then the finite expansion for μ is only an approximation.

A set of testing functions is selected w_m in the domain of L. The inner product of $L(\mu) = s$ is evaluated for each w_m. Therefore, we have

$$\langle W_m, L(\mu) \rangle = \langle W_m, \sum_{n=1}^{N} a_n L(\mu_n) \rangle$$

or

$$\langle W_m, s \rangle = \sum_{n=1}^{N} a_n \langle W_m, L(\mu_n) \rangle. \qquad (2\text{-}28)$$

The resulting set of linear algebraic equations can then be solved for the unknown coefficients.

The method used here is a special case of the method of moments. The testing functions selected are the same as the basis functions. In this case the method of mements is properly called Galerkin's method.

The unknown function in the case of equation (2-27) is the charge distribution $\sigma(x)$. The exact solution is given for a microstrip in free space over a ground plane as

$$\sigma(x) = \frac{A}{\sqrt{1 - [\frac{2x}{w}]^2}} .$$

A is a constant determined by the potential of the strip with respect to the ground plane. For the perturbed strip over a dielectric substrate in the presence of another strip, variational terms can be added to give a good approximation of the charge distribution.

The basis functions selected in this case are

$$6(x) = \frac{A}{\sqrt{1 - [\frac{2(x-s)}{w}]^2}} + \frac{B(x-s)}{\sqrt{1 - [\frac{2(x-s)}{w}]^2}} \qquad (2\text{-}29)$$

where $s = \frac{a+b}{2}$.

The testing functions are the same as the basis functions since the basis functions can be integrated analytically. More terms could be added for more accuracy, but the analytical complexity increases rapidly.

The charge distribution must be calculated for both the even and odd order cases. Let the even order voltage distribution be given as

$$V_{strip}{}^1 = V_{strip}{}^2 = 1 \text{ volt},$$

and the odd order voltage distribution be given as

$$V_{strip}{}^1 = 1 \text{ volt}$$

$$V_{strip}{}^2 = -1 \text{ volt}.$$

Due to the symmetry of the problem, the integration as shown in equation (2-26) need only be done for strip 2. Using equations (2-27) and (2-28) we have for the even order case,

$$\int_a^b \frac{1}{\sqrt{1 - [\frac{2(x-s)}{w}]^2}}\, dx = \frac{2A_1}{\pi\varepsilon_o} \int_o^\infty \frac{F(\alpha)}{\alpha} \int_a^b \frac{\cos x'}{\sqrt{1 - [\frac{2(x'-s)}{w}]^2}}\, dx'$$

$$\cdot \int_a^b \frac{\cos\alpha x}{\sqrt{1 - [\frac{2(x-s)}{w}]^2}}\, dx d\alpha$$

$$+ \frac{2B1}{\pi\varepsilon_o} \int_o^\infty \frac{F(\alpha)}{\alpha} \int_a^b \frac{(x'-s)\cos\alpha x'}{\sqrt{1 - [\frac{2(x'-s)}{w}]^2}} dx' \int_a^b \frac{\cos\alpha x}{\sqrt{1 - [\frac{2(x-s)}{w}]^2}} dx d\alpha$$

(2-30)

and

$$\int_a^b \frac{x-s}{\sqrt{1 - [\frac{2(x-s)}{w}]^2}} dx = \frac{2A_1}{\pi\varepsilon_o} \int_o^\infty \frac{F(\alpha)}{\alpha} \int_a^b \frac{\cos\alpha x'}{\sqrt{1 - [\frac{2(x-s)}{w}]^2}} dx' \int_a^b \frac{(x-s)\cos\alpha x}{\sqrt{1 - [\frac{2(x-s)}{w}]^2}} dx d\alpha$$

$$+ \frac{2B_1}{\pi\varepsilon_o} \int_o^\infty \frac{F(\alpha)}{\alpha} \int_a^b \frac{(x'-s)\cos\alpha x'}{\sqrt{1-[\frac{2(x'-s)}{w}]}} dx' \int_a^b \frac{(x-s)\cos\alpha x}{\sqrt{1-[\frac{2(x-s)}{w}]^2}} dx d\alpha \quad (2-31)$$

Similarly for the odd order case,

$$\int_a^b \frac{-1}{\sqrt{1-[\frac{2(x-s)}{w}]^2}} dx = \frac{2A_2}{\pi\varepsilon_o} \int_o^\infty \frac{F(\alpha)}{\alpha} \int_a^b \frac{\sin\alpha x'}{\sqrt{1-[\frac{2(x'-s)}{w}]}} dx' \int_a^b \frac{\sin\alpha x}{\sqrt{1-[\frac{2(x-s)}{w}]^2}} dx d\alpha$$

$$+ \frac{2B_2}{\pi\varepsilon_o} \int_o^\infty \frac{F(\alpha)}{\alpha} \int_a^b \frac{(x'-s)\sin\alpha x'}{\sqrt{1-[\frac{2(x'-s)}{w}]^2}} dx' \int_a^b \frac{\sin\alpha x}{\sqrt{1-[\frac{2(x-s)}{w}]^2}} dx d\alpha \quad (2-32)$$

and,

$$- \int_a^b \frac{x-s}{\sqrt{1-[\frac{2(x-s)}{w}]^2}} dx = \frac{2A_2}{\pi\varepsilon_o} \int_o^\infty \frac{F(\alpha)}{\alpha} \int_a^b \frac{\sin\alpha x'}{\sqrt{1-[\frac{2(x'-s)}{w}]^2}} dx' \int_a^b \frac{(x-s)\sin\alpha x}{\sqrt{1-[\frac{2(x-s)}{w}]^2}} dx d\alpha$$

$$+ \frac{2B_2}{\pi t_o} \int_o^\infty \frac{F(\alpha)}{\alpha} \int_a^b \frac{(x'-s)\sin\alpha x'}{\sqrt{1-[\frac{2(x'-s)}{w}]^2}} dx' \int_a^b \frac{(x-s)\sin\alpha x}{\sqrt{1-[\frac{2(x-s)}{w}]^2}} dx d\alpha \quad (2-33)$$

Several of these integrals can be analytically integrated and are given as follows

$$\int_a^b \frac{1}{\sqrt{1-[\frac{2(x-s)}{w}]^2}} dx = \frac{\pi w}{2} = P_1 \quad (2-34)$$

$$\int_a^b \frac{x-s}{\sqrt{1-\left[\frac{2(x-s)}{w}\right]^2}}\,dx = 0 \tag{2-35}$$

$$\int_a^b \frac{\cos \alpha x'}{\sqrt{1-\left[\frac{2(x'-s)}{w}\right]^2}}\,dx' = \frac{\pi w}{2}\cos(\alpha s)J_o\left(\frac{\alpha w}{2}\right) = P_2 \tag{2-36}$$

$$\int_a^b \frac{(x-s)\cos\alpha x}{\sqrt{1-\left[\frac{2(x-s)}{w}\right]^2}}\,dx = -\frac{\pi w^2}{4}\sin(\alpha s)J_1\left(\frac{w\alpha}{2}\right) = P_3 \tag{2-37}$$

$$\int_a^b \frac{\sin \alpha x}{\sqrt{1-\left[\frac{2(x-s)}{w}\right]^2}}\,dx = \frac{\pi w}{2}\sin(\alpha s)J_o\left(\frac{\alpha w}{2}\right) = P_4 \tag{2-38}$$

$$\int_a^b \frac{(x-s)\sin\alpha x}{\sqrt{1-\left[\frac{2(x-s)}{w}\right]^2}}\,dx = \frac{\pi w^2}{4}\cos(\alpha s)J_1\left(\frac{w\alpha}{2}\right) = P_5. \tag{2-39}$$

From equations (2-30) through (2-33) and equations (2-34) through (2-39) we have

$$P_1 = \frac{2A_1}{\pi\varepsilon_o}\int_o^\infty \frac{F(\alpha)}{\alpha}P_2^2\,d\alpha + \frac{2B_1}{\pi\varepsilon_o}\int_o^\infty \frac{F(\alpha)}{\alpha}P_3P_2\,d\alpha \tag{2-40}$$

$$0 = \frac{2A_1}{\pi\varepsilon_o}\int_o^\infty \frac{F(\alpha)}{\alpha}P_2P_3\,d\alpha + \frac{2B_1}{\pi\varepsilon_o}\int_o^\infty \frac{F(\alpha)}{\alpha}P_3^2\,d\alpha \tag{2-41}$$

$$-P_1 = \frac{2A_2}{\pi\varepsilon_o}\int_o^\infty \frac{F(\alpha)}{\alpha}P_4^2\,d\alpha + \frac{2B_2}{\pi\varepsilon_o}\int_o^\infty \frac{F(\alpha)}{\alpha}P_5P_4\,d\alpha \tag{2-42}$$

$$0 = \frac{2A_2}{\pi\varepsilon_o}\int_o^\infty \frac{F(\alpha)}{\alpha}P_4P_5\,d\alpha + \frac{2B_2}{\pi\varepsilon_o}\int_o^\infty \frac{F(\alpha)}{\alpha}P_5^2\,d\alpha \tag{2-43}$$

Six different integrals must be solved in this set of equations in order to solve for the unknown coefficients. The integrals were first evaluated directly using the IMSL computer subroutine DCADRE. The cost of evaluating these integrals

was too high because of slow convergence for each integral. Asymptotic approximations of the six functions to be integrated can be found in a table of integrals [9] and are given as follows:

$$\int_0^\infty \frac{F(\alpha)}{\alpha} P_2{}^2 d\alpha \rightarrow$$

$$\frac{\pi w}{4(\varepsilon r+1)} \int_0^\infty \frac{\cos 2\alpha s \sin w\alpha + \cos 2\alpha s + \sin(w\alpha) + 1}{\alpha^2 + \beta^2} d\alpha$$

$$= \frac{\pi w}{4(\varepsilon r+1)} \{\frac{\pi}{2\beta} e^{-2s\beta} + \frac{1}{2\beta}[e^{-w\beta}\overline{E}_i(w\beta) - e^{w\beta}E_i(-w\beta)]$$

$$+ \frac{\pi}{2\beta} + \frac{1}{4\beta} e^{-w\beta}\{e^{2s\beta}E_i[\beta(w-2s)] + e^{-2s\beta}E_i[\beta(w+2s)]\}$$

$$- \frac{1}{4\beta} e^{w\beta}\{e^{2s\beta}E_i[-\beta(w+2s)] + e^{-2s\beta}E_i[\beta(2s-w)]\} \} \qquad (2\text{-}44)$$

$$\int_0^\infty \frac{F(\alpha)}{\alpha} P_3 P_2 d\alpha \rightarrow$$

$$\frac{w^2\pi}{8(\varepsilon r+1)} \int_0^\infty \frac{\sin 2\alpha s \cos(w\alpha)}{\alpha^2 + \beta^2} d\alpha$$

$$= \frac{w^2\pi}{8(\varepsilon r+1)} \{\frac{1}{4\beta} e^{-2s\beta}\{e^{w\beta}E_i[\beta(2s-w)] + e^{-w\beta}E_i[\beta(2s+w)]\}$$

$$- \frac{1}{4\beta} e^{2s\beta}\{e^{w\beta}E_i[-\beta(2s+w)] + e^{-w\beta}E_i[\beta(w-2s)]\} \} \qquad (2\text{-}45)$$

$$\int_0^\infty \frac{F(\alpha)}{\alpha} P_3{}^2 d\alpha \rightarrow$$

$$\frac{w^4\pi^2}{16(\varepsilon r+1)} \frac{4}{\pi w} \int_0^\infty \frac{1 - \sin w\alpha - \cos 2\alpha s + \cos 2\alpha s \sin w\alpha}{\alpha^2 + \beta^2} d\alpha$$

$$= \frac{w^3\pi}{16(\varepsilon r+1)} \{\frac{\pi}{2\beta} - \frac{1}{2\beta}[e^{-w\beta}\overline{E}_i(w\beta) - e^{w\beta}E_i(-w\beta)] - \frac{\pi}{2\beta} e^{-2s\beta}$$

$$+ \frac{1}{4\beta} e^{-w\beta}\{e^{2s\beta}E_i[\beta(w-2s)] + e^{-2s\beta}E_i[\beta(w+2s)]\}$$

$$- \frac{1}{4\beta} e^{w\beta}\{e^{2s\beta}E_i[-\beta(w+2s)] + e^{-2s\beta}E_i[\beta(2s-w)]\}\} \qquad (2\text{-}46)$$

$$\int_o^\infty \frac{F(\alpha)}{\alpha} P_4{}^2 d\alpha \rightarrow$$

$$\frac{\pi w}{4(\varepsilon r+1)} \int_o^\infty \frac{1 + \sin w\alpha - \cos 2\alpha s - \cos 2\alpha s \sin w\alpha}{\alpha^2 + \beta^2} d\alpha$$

$$= \frac{\pi w}{4(\varepsilon r+1)} \{\frac{\pi}{2\beta} + \frac{1}{2\beta}[e^{-w\beta}\overline{E_i}(w\beta) - e^{w\beta} E_i(-w\beta)] - \frac{\pi}{2\beta} e^{-2s\beta}$$

$$- \frac{1}{4\beta} e^{-w\beta}\{e^{2s\beta}E_i[\beta(w-2s)] + e^{-2s\beta}E_i[\beta(w-2s)]\} \qquad (2\text{-}47)$$

$$\int_o^\infty \frac{F(\alpha)}{\alpha} P_5 P_4 d\alpha \rightarrow$$

$$\frac{w^2\pi}{8(\varepsilon r+1)} \int_o^\infty \frac{\sin 2\alpha s \cos(w\alpha-\pi)}{\alpha^2 + \beta^2} d\alpha$$

$$= - \frac{w^2\pi}{8(\varepsilon r+1)} \{\frac{1}{4\beta} e^{-2s\beta}\{e^{w\beta}E_i[\beta(2s-w)] + e^{-w\beta}E_i[\beta(2s+w)]\}$$

$$- \frac{1}{4\beta} e^{2s\beta}\{e^{w\beta}E_i[-\beta(2s+w)] + e^{-w\beta}E_i[\beta(w-2s)]\}\} \qquad (2\text{-}48)$$

$$\int_o^\infty \frac{F(\alpha)}{\alpha} P_5{}^2 d\alpha \rightarrow$$

$$(\frac{w^2\pi}{4})^2 \frac{4}{(\varepsilon r+1)\pi w} \int_o^\infty \frac{1 - \sin w\alpha + \cos 2\alpha s - \cos 2\alpha s \sin w\alpha}{\alpha^2 + \beta^2} d\alpha$$

$$= \frac{w^3\pi}{16}(\frac{1}{\varepsilon r+1}) \frac{\pi}{2\beta} - \frac{1}{2\beta}[e^{-w\beta}\overline{E_i}(w\beta) - e^{w\beta}E_i(-w\beta)] + \frac{\pi}{2\beta} e^{-2s\beta}$$

$$- \frac{1}{4\beta} e^{-w\beta}\{e^{2s\beta}E_i[\beta(w-2s)] + e^{-2s\beta}E_i[\beta(w+2s)]\}$$

$$+ \frac{1}{4\beta} e^{w\beta}\{e^{2s\beta}E_i[-\beta(w+2s)] + e^{-2s\beta}E_i[\beta(2s-w)]\}\} \qquad (2\text{-}49)$$

In each equation, β is a constant that was added to the denominator so that each integral could be calculated analytically.

The accuracy of each equation is therefore dependent on small β. The method to calculate each integral is given as follows.

Let $A(\alpha)$ be the asymptotic approximation of the function $f(\alpha)$ to be integrated. Then the integral can be approximated as

$$I = \int_0^{\Delta\alpha} f(\alpha) - A(\alpha)\,d\alpha + \int_0^{\infty} A(\alpha)\,d\alpha.$$

The first part of the integration was done on the computer using the IMSL subroutine DCADRE. The second part of the integration could in each case be calculated analytically. $\Delta\alpha$ was taken large enough so as to ensure good convergence of the sum of the two integrals. The cost of evaluating these integrals using this method was found to be low without much loss of accuracy as compared to the exact form.

Once the six integrals given in equations (2-40) through (2-43) have been calculated, then the constant coefficients of the basis functions are easily determined.

Let

$$I_1 = \frac{2}{\pi\varepsilon_0} \int_0^{\infty} \frac{F(\alpha)}{\alpha} P_2^2\,d\alpha$$

$$I_2 = \frac{2}{\pi\varepsilon_0} \int_0^{\infty} \frac{F(\alpha)}{\alpha} P_3 P_2\,d\alpha$$

$$I_3 = \frac{2}{\pi\varepsilon_0} \int_0^{\infty} \frac{F(\alpha)}{\alpha} P_3^2\,d\alpha$$

$$I_4 = \frac{2}{\pi\varepsilon_0} \int_0^{\infty} \frac{F(\alpha)}{\alpha} P_4^2\,d\alpha$$

$$I_5 = \frac{2}{\pi\varepsilon_o}\int_o^\infty \frac{F(\alpha)}{\alpha} P_4 P_5 d\alpha$$

$$I_6 = \frac{2}{\pi\varepsilon_o}\int_o^\infty \frac{F(\alpha)}{\alpha} P_5^2 d\alpha$$

Then we have for the even mode

$$\begin{bmatrix} \frac{\pi w}{2} \\ 0 \end{bmatrix} = \begin{bmatrix} I_1 & I_2 \\ I_2 & I_3 \end{bmatrix} \begin{bmatrix} A_1 \\ B_1 \end{bmatrix} \tag{2-50}$$

and for the odd mode

$$\begin{bmatrix} -\frac{\pi w}{2} \\ 0 \end{bmatrix} = \begin{bmatrix} I_4 & I_5 \\ I_5 & I_6 \end{bmatrix} \begin{bmatrix} A_2 \\ B_2 \end{bmatrix} . \tag{2-51}$$

These equations are easily solved by either matrix inversion or algebraic manipulation.

2.3 Capacitance Coefficients

The total charge on the conductor is given as

$$Q = \int_a^b \sigma(x)\,dx.$$

This integral is easily evaluated for both the even and odd modes. We have for the even mode

$$Q^{(1)} = \int_a^b \frac{A_1}{\sqrt{1-[\frac{2(x-s)}{w}]^2}} + \frac{B_1(x-s)}{\sqrt{1-[\frac{2(x-s)}{w}]^2}}\,dx$$

$$= A_1(\tfrac{\pi w}{2}) + B_1(0) \tag{2-52}$$

and similarly for the odd mode

$$Q^{(2)} = A_2(\tfrac{\pi W}{2}) + B_2(0). \qquad (2\text{-}53)$$

In a multiconductor transmission line with transverse fields [10]

$$Q_i = \sum_{j=1}^{n} C_{ij} V_j$$

where C_{ij} are Maxwell's capacitance coefficients. In our case n=2 so that we have for the even mode

$$\begin{bmatrix} Q_1^{(1)} \\ Q_2^{(1)} \end{bmatrix} = \begin{bmatrix} C_{11} & C_{12} \\ C_{21} & C_{22} \end{bmatrix} \begin{bmatrix} 1 \\ 1 \end{bmatrix} \qquad (2\text{-}54)$$

and for the odd mode

$$\begin{bmatrix} Q_1^{(2)} \\ Q_2^{(2)} \end{bmatrix} = \begin{bmatrix} C_{11} & C_{12} \\ C_{21} & C_{22} \end{bmatrix} \begin{bmatrix} 1 \\ -1 \end{bmatrix} \qquad (2\text{-}55)$$

Using the symmetry of the problem the charges on the two strips are related by

$$Q_1^{(1)} = Q_2^{(1)}$$

$$Q_1^{(2)} = -Q_2^{(2)}.$$

Equations (2-54) and (2-55) together with these conditions can then be used to solve for the capacitance coefficients.

2.4 Formulation of the Integral Relating Inductance and Current

The formulation here is much the same as that given for the charge voltage integral equation. Figure 1 shows the geometry of the problem. From equation (2-2) the transverse $\bar{H}$ fields are given as

$$H_t^{(2)} = \int_{-\infty}^{\infty} I_1^{(2)} \left[\frac{\hat{x}(-\beta_o) + \hat{y}(\alpha)}{\sqrt{\alpha^2 + \beta^2}}\right] \frac{j}{\sqrt{2\pi}} e^{-j\alpha x} d\alpha e^{-j\beta_o y}$$

$$+ \int_{-\infty}^{\infty} I_2^{(2)} \left[\frac{\hat{x}(\alpha) + \hat{y}(\beta_o)}{\sqrt{\alpha^2 + \beta^2}}\right] \frac{j}{2\pi} e^{-j\alpha x} d\alpha e^{-j\beta_o y}$$

where $I_1^{(2)}$ and $I_2^{(2)}$ are as given in equation (2-15).

Since it is desired to find the flux linking the ground plane to the strip, then only the $\hat{x}$ component of the $\bar{H}$ field is needed. Applying the zero frequency approximation we have

$$H_x^{(2)} = \int_{-\infty}^{\infty} \alpha \, I_2^{(2)} \frac{j}{\sqrt{2\pi}} \frac{1}{|\bar{k}|} e^{-j\alpha x} d\alpha \qquad (2\text{-}56)$$

where

$$I_2^{(2)} = \frac{\cosh(|\alpha|(t+z)) \; i_2(\alpha)}{\cosh(|\alpha|t) + \sinh(|\alpha|t) \coth(|\alpha|d)} .$$

Let d go to infinity so that

$$I_2^{(2)} = \frac{\cosh(|\alpha|(t+z)) \; i_2(\alpha)}{\cosh(|\alpha|t) + \sinh(|\alpha|t)}$$

where $i_2(\alpha)$ is given as

$$i_2(\alpha) = \int_{-\infty}^{\infty} \frac{j}{\sqrt{2\pi}} e^{j\alpha x} \, i_y(x') dx' .$$

The flux linking the strip to the ground plane is

$$\Phi(x) = \int_{-t}^{0} \mu_o H_x dz$$

$$= \frac{\mu_o}{2\pi} \int_{-\infty}^{\infty} \int_{-t}^{0} \alpha \frac{\cosh(|\alpha|(t+z))}{\cosh(|\alpha|t) + \sinh(|\alpha|t)} \frac{1}{|\alpha|} dz$$

$$\cdot i_y(x') e^{-j\alpha(x-x')} dx' d\alpha$$

$$= \frac{\mu_o}{2\pi} \int_{-\infty}^{\infty} \frac{\alpha}{|\alpha|^2} \frac{1}{\coth(|\alpha|t) + 1} i_y(x') e^{-j\alpha(x-x')} dx' d\alpha \qquad (2\text{-}57)$$

Using the symmetry of the problem we finally have

$$\Phi(x) = \int_{o}^{\infty} \int G(\alpha, x|x') i_y(x') dx' d\alpha \qquad (2\text{-}58)$$

where

$$G(\alpha, x|x') = \frac{2\mu_o}{\pi} \frac{F(\alpha)}{\alpha} \cos \alpha x \cos \alpha x' \qquad (2\text{-}59)$$

for the even mode and

$$G(\alpha, x|x') = \frac{2\mu_o}{\pi} \frac{F(\alpha)}{\alpha} \sin \alpha x \sin \alpha x'$$

for the odd mode and

$$F(\alpha) = \frac{1}{\coth(\alpha t) + 1} .$$

That this equation is very similar to the one given for voltage on the strip should not be surprising since the two problems are dual to each other. Therefore, the same technique used to solve for the charge distribution on one strip due to a voltage on the strip can also be used to solve

for the current distribution on the strip due to a flux linking the strip with ground.

2.5 Inductance Coefficients

To find the current distribution on the strip, the same method is used as that used for finding the charge distribution. Once the current distribution is known then the total current is found by

$$I = \int_a^b i_y(x)\,dx.$$

In an N conductor transmission system, the magnetic flux linking the $n^{\underline{th}}$ conductor and ground is the resultant of currents flowing in the N independent conductors [10]

$$\Phi_n = (L_{nm})\,I_m$$

where the L_{nm} are the line coefficients of inductance. In finding the currents on a strip, the magnetic flux was assumed to have a certain value

$$\Phi_1 = \Phi_2 = 1$$

for the even case and

$$\Phi_1 = 1,\ \Phi_2 = -1$$

for the odd case. Therefore, for the even case

$$\begin{bmatrix} 1 \\ 1 \end{bmatrix} = \begin{bmatrix} L_{11} & L_{12} \\ L_{21} & L_{22} \end{bmatrix} \begin{bmatrix} I_1^{(1)} \\ I_2^{(1)} \end{bmatrix} \qquad (2\text{-}60)$$

and for the odd case

$$\begin{bmatrix} 1 \\ \\ -1 \end{bmatrix} = \begin{bmatrix} L_{11} & L_{12} \\ \\ L_{21} & L_{22} \end{bmatrix} \begin{bmatrix} I_1^{(2)} \\ \\ I_2^{(2)} \end{bmatrix} . \qquad (2\text{-}61)$$

Again using the symmetry of the problem, the currents on the strips are related by

$$I_1^{(1)} = I_2^{(1)}$$

for the even case and

$$-I_1^{(2)} = I_2^{(2)}$$

for the odd case. Equations (2-60) and (2-61) together with these conditions can then be solved for the inductance coefficients.

3. D. C. TRANSIENT ANALYSIS OF COUPLED LOSSLESS TRANSMISSION LINES

The D. C. transient analysis of coupled microstrip transmission lines is covered in detail in the literature. In this thesis an effort has been made to apply these techniques to real world digital circuits. The loads are the digital devices and the transmission line is the microstrip conductor connecting two devices on a printed circuit board. The output and input impedances of digital circuits are highly non-linear and the reflections from these types of loads can cause distortion to the original signal so that false switching of the receiving-device may occur. In addition, coupling to adjacent lines occurs from the drive-line which can cause false switching to occur on the non-drive-lines. In this chapter a method is presented which can be used to calculate distortion from both coupling and reflections.

3.1 Eigenmode Expansion Method for Multi-Conductor Transmission Lines

Several papers [2,3,4] were published during the 60's and early 70's on crosstalk between conductors in three wire transmission line systems. The models used are not easily extendable to more than three conductor transmission lines and do not take into account reflections from the terminating impedances. Recently, some techniques using eigenmode expansion

methods have been presented [5,6]. The advantage of a modal analysis technique is that an N conductor transmission line system can be modeled as a single tube terminated by a network through which N modes of propagation are possible.

We begin by defining the following matrices which give the line voltages and currents of the system (fig. 3) and the capacitance and inductance coefficients coupling those lines.

$$[V(y,t)] = \begin{bmatrix} V_1(y,t) \\ \vdots \\ V_N(y,t) \end{bmatrix} \tag{3-1}$$

$$[I(y,t)] = \begin{bmatrix} i_1(y,t) \\ \vdots \\ i_N(y,t) \end{bmatrix} \tag{3-2}$$

$$[L] = \begin{bmatrix} L_{11} & \cdots & L_{1N} \\ \vdots & & \\ L_{N1} & \cdots & L_{NN} \end{bmatrix} \tag{3-3}$$

$$[C] = \begin{bmatrix} C_{11} & \cdots & C_{1N} \\ \vdots & & \\ C_{N1} & \cdots & C_{NN} \end{bmatrix} \tag{3-4}$$

The telegrapher equations for an N+1 conductor transmission line system are given as

$$\frac{\alpha}{\alpha y}[V(y,t)] = -[L]\frac{\alpha}{\alpha t}[I(y,t)] \tag{3-5a}$$

$$\frac{\alpha}{\alpha y}(I(y,t)] = -[C]\frac{\alpha}{\alpha t}[V(y,t)]. \tag{3-5b}$$

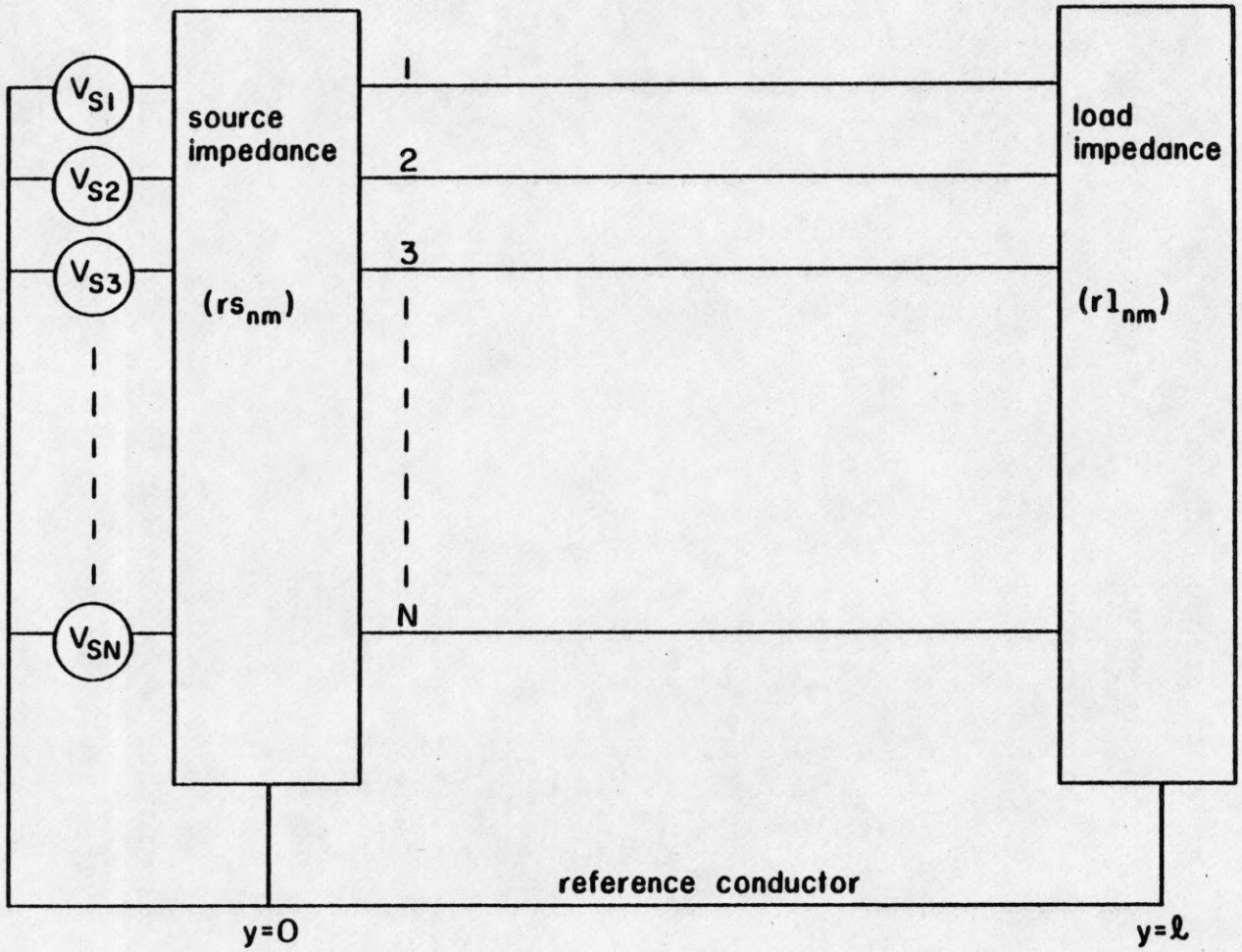

Figure 3 - Multiconductor Transmission Line System

Equations (3-5) can then be combined to give the wave equations for both voltage and current,

$$\frac{\alpha^2}{\alpha y^2}[V(y,t)] = [L][C]\frac{\alpha^2}{\alpha t^2}[V(y,t)] \tag{3-6a}$$

$$\frac{\alpha^2}{\alpha y^2}[I(y,t)] = [C][L]\frac{\alpha^2}{\alpha t^2}[I(y,t)]. \tag{3-6b}$$

It should be stressed that these equations are for a TEM mode of propagation only. At high frequencies the mode of propagation is not TEM for a microstrip structure. However, at low frequencies the propagation is very nearly TEM so that very good calculations can be gained with this method.

Now, define matrices for generator voltages and source and load impedances.

$$[R_S] = \begin{bmatrix} rS_{11} & \cdots & rS_{1N} \\ \vdots & & \\ rS_{N1} & & rS_{NN} \end{bmatrix}, \tag{3-7}$$

$$[R_L] = \begin{bmatrix} r\ell 11 & \cdots & r\ell 1N \\ \vdots & & \\ r\ell N1 & & r\ell NN \end{bmatrix}, \tag{3-8}$$

$$[V_S(t)] = \begin{bmatrix} V_{S1} \\ \vdots \\ V_{SN} \end{bmatrix}. \tag{3-9}$$

The source and load matrices describe the networks that terminate each end of the system (fig. 3), and the source matrix gives a description of all the generators at the y=0 end of the system.

Solutions to (3-6) are given as

$$[V(y,t)] = [V_o] \cdot g(t \pm \frac{y}{v}) \qquad (3\text{-}10a)$$

$$[I(y,t)] = [I_o] \cdot g(t \pm \frac{y}{v}) \qquad (3\text{-}10b)$$

The variable v is the wave velocity. A positive sign in front of $\frac{y}{v}$ denotes a wave propagating in the negative y direction and a negative sign denotes a wave propagating in the positive y direction. Now we substitute (3-10a) into (3-6a) to get

$$\frac{1}{v^2}[V_o]\ g\ (t \pm \frac{y}{v}) = [L][C][V_o]\ g\ (t \pm \frac{y}{v}). \qquad (3\text{-}11)$$

Equation (3-11) is an eigenvalue equation where $\frac{1}{v_m^2}$ are the eigenvalues and $[V_o{}^{(m)}]$ are the eigenvectors. Since for an N conductor transmission line system [L][C] is an NxN matrix, then there will be N eigenvalues (not necessarily distinct) and N eigenvectors. The eigenvalues and eigenvectors are related to the modes of the system, each mode having a velocity $\frac{1}{v_m}$ and amplitude $[V_o{}^{(m)}]$. Thus we can model our system of N conductors as a single tube with N modes of propagation. Similarly, from equations (3-10b) and (3-6b) an eigenvalue equation for the

currents can be found with $\frac{1}{v_m^2}$ again being the eigenvalues and $[I_o^{(m)}]$ being the eigenvectors corresponding to the eigenvalues.

Let

$$[S_v] = \{[V_o^{(1)}], [V_o^{(2)}], \ldots, [V_o^{(N)}]\} \tag{3-12}$$

and

$$[S_I] = \{[I_o^{(1)}], [I_o^{(2)}], \ldots, [I_o^{(N)}]\} . \tag{3-13}$$

From equation (3-5a) the modal voltages and currents are related by

$$[V_o^m] = \frac{1}{v_m} [L][I_o^m]$$

or from (3-12) and (3-13)

$$[S_I] = [L]^{-1}[S_v][\Lambda] \tag{3-14}$$

where $[\Lambda]$ is a diagonal matrix whose elements are the eigenvalues $\frac{1}{v_m}$ of the matrix $[L][C]$.

The total voltage at any point on the line is the sum of the incident and reflected voltages

$$[V(y,t)] = [V_{inc}(y,t)] + [V_{ref}(y,t)] .$$

Thus, the modal voltages can be related to the conductor voltages by

$$[V(y,t)] = [S_v]\left\{\begin{bmatrix} g(t-\frac{y}{v_1}) \\ g(t-\frac{y}{v_N}) \end{bmatrix} + \begin{bmatrix} g(t+\frac{y}{v_1}) \\ g(t+\frac{y}{v_N}) \end{bmatrix}\right\}$$

$$= S_v\{[F_{inc}(y,t)]+[F_{ref}(y,t)]\}. \qquad (3\text{-}15)$$

This is a general equation that has not been subject to any boundary conditions.

We now develop the idea of a characteristic impedance matrix. By definition

$$[V(y,t)] = [ZC][I(y,t)]$$

for the line voltages and

$$[S_v] = [ZC][S_I] \qquad (3\text{-}16)$$

for the modal voltages. Substitute (3-14) into (3-16) to get

$$[ZC] = [S_v][S_I]^{-1}$$

$$= [S_v][\Lambda]^{-1}[S_v]^{-1}[L]. \qquad (3\text{-}17)$$

From equation (3-15) the voltages anywhere on the line can be found, but the main interest in our case is to find the voltages at either end of the line. At y=o

$$[V(o,t)] = [S_v]\{[F_{inc}(o,t)] + [F_{ref}(o,t)]\}. \qquad (3\text{-}18)$$

Since the generator voltages are located at y=o, then we can write

$$[V_{inc}(o,t)] = [\tau_s][V_s(o,t)] + [\rho_s][V_{ref}(o,t)] \qquad (3\text{-}19)$$

where τ_s and ρ_s are the transmission and reflection coefficients at the source end, respectively. $[\tau_s]$ and $[\rho_s]$ are defined by

$$[\tau_s] = [ZC]\{[R_s] + [ZC]\}^{-1} \qquad (3\text{-}20)$$

and

$$[\rho_s] = \{[R_s] - [ZC]\}\cdot\{[R_s] + [ZC]\}^{-1}. \qquad (3\text{-}21)$$

From (3-18) and (3-19)

$$[S_v][F_{inc}(o,t)] = [\tau_s][V_s(o,t)] + [\rho_s][V_{ref}(o,t)]$$

or

$$[F_{inc}(o,t)] = [S_v]^{-1}[\tau_s][V_s(o,t)] + [S_v]^{-1}[\rho_s] \cdot [V_{ref}(o,t)]$$

$$= [S_v]^{-1}[\tau_s][V_s(o,t)] + [S_v]^{-1}[\rho_s] \cdot [S_v][F_{ref}]. \qquad (3\text{-}22)$$

Let

$$[\tau_s^{(m)}] = [S_v]^{-1}[\tau_s] \qquad (3\text{-}23)$$

and

$$[\rho_s^{(m)}] = [S_v]^{-1}[\rho_s][S_v] \tag{3-24}$$

be the modal reflection and transmission coefficients at the source end. Then (3-22) can be written

$$[F_{inc}(o,t)] = [\tau_s^{(m)}][V_s(o,t)] + [\rho_s^{(m)}][F_{ref}(o,t)]. \tag{3-25}$$

Similarly, at the load end of the line

$$[V(l,t)] = [S_v]\{[F_{inc}(l,t)] + [F_{ref}(l,t)]\}. \tag{3-26}$$

Now

$$[V_{ref}(l,t)] = [\rho_L][V_{inc}(l,t)] \tag{3-27}$$

where $[\rho_L]$ is the voltage reflection coefficient matrix at the load end of the line given by

$$[\rho_L] = \{[R_L] - [ZC]\}\cdot\{[R_L] + [ZC]\}^{-1}. \tag{3-28}$$

From (3-26) and (3-27)

$$[S_v][F_{ref}(l,t)] = [\rho_L][V_{inc}(l,t)]$$

or

$$[F_{ref}(l,t)] = [S_v]^{-1}[\rho_L][V_{inc}(l,t)]. \tag{3-29}$$

Thus, we can define the modal reflection coefficient matrix at the load end of the system by

$$[\rho_L^{(m)}] = [S_v]^{-1}[\rho_L]. \tag{3-30}$$

Therefore,

$$[F_{ref}(l,t)] = [\rho_L^{(m)}][F_{inc}(l,t)]. \tag{3-31}$$

It can be seen that once the source voltage matrix, the terminating impedances and the inductance and capacitance coefficient matrices are known, then we can find the voltages on the lines in our system.

4. RESULTS

From the equations developed in chapters 2 and 3, a program was written to evaluate the voltages on both ends of a system of two parallel microstrip transmission lines with any type of resistive loads. This chapter gives some results from that program as well as some experimental results.

4.1 Assumptions and Simplifications.

We would like to be able to find the response of a system to a pulse with finite fall and rise times (figure 4). For computational purposes an approximation to this pulse can be used where the voltage ramps at the beginning and end of the pulse can be approximated by a series of positive and negative going voltage steps, each with an amplitude and length determined by the rise time and amplitude of the original pulse (figure 5). The time between steps, Δt, is given by the rise time divided by some constant c. Similarly, the amplitude, Δv, of each step is given by the amplitude, V_o, of the original pulse divided by the same constant c. The larger the constant c, the better the approximation becomes.

Therefore, our problem essentially becomes one of exciting the transmission line system with a series of step

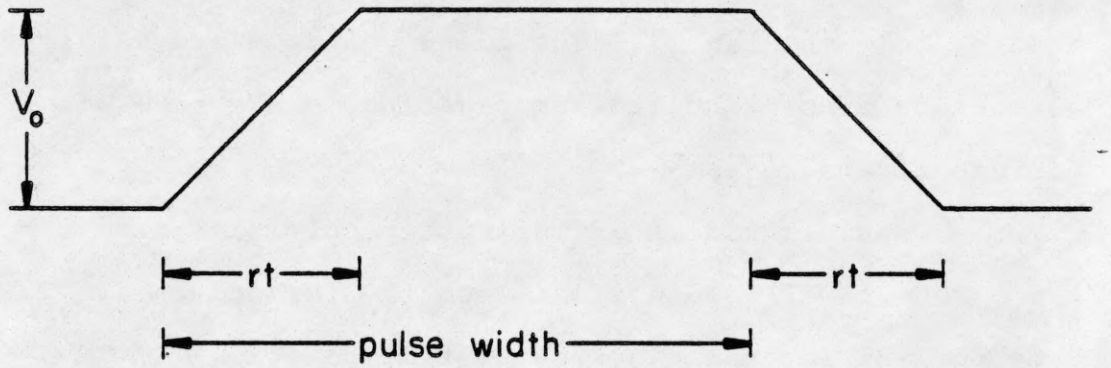

Figure 4 - Input Pulse

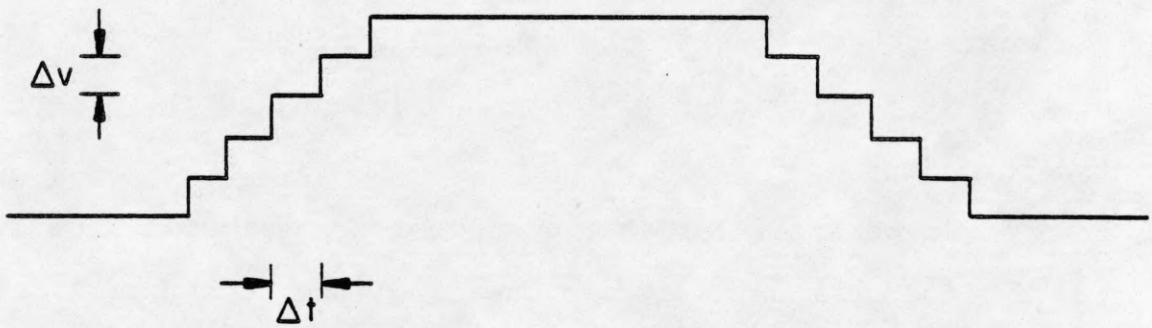

Figure 5 - Approximation to Input Pulse

functions. From equation 3-25, it can be seen that both modes of the system will be excited by a unit step generated on only one line. These model voltages can be viewed as voltage discontinuities propagating down a tube with different velocities.

Consider mode 1 of our system only. At time $t = 1/v_1$, mode 1 will be incident upon the far end load. Expanding 3-31 for the two line system,

$$\begin{bmatrix} F_{2ref}(1,\ 1/v_1) \\ F_{2ref}(1,\ 1/v_1) \end{bmatrix} = \begin{bmatrix} \rho_{L11}^{(m)} & \rho_{L12}^{(m)} \\ \rho_{L21}^{(m)} & \rho_{L22}^{(m)} \end{bmatrix} \begin{bmatrix} F_1 inc(1,1/v_1) \\ 0 \end{bmatrix} \qquad (4\text{-}1)$$

it can be seen that both modes will be reflected back even though only one mode has been incident on the far end load. After both modal voltage discontinuities have been incident on the far end load, four voltage discontinuities will be propagating back towards the source end of the tube. Two voltage discontinuities will be in mode one and the other two in mode two.

In general, for an N conductor transmission line system excited by a unit step on one line, the number of voltage discontinuities all propagating in the same direction down a tube for a single mode is

$$N_m = (N - 1) \cdot N_{ref} + 1 \qquad (4\text{-}2)$$

where

N_m = number of voltage discontinuities existing along a tube for the mth mode

N_{ref} = number of reflections that have occurred for all the modes.

It can be seen that as time goes on, an expanding amount of computer memory will be needed for the bookkeeping-so to speak. In the current version of the program none of the cross-coupled modes are propagated back down the tube past the second reflection. The results to be presented show where this approximation may or may not work.

4.2 Brief Program Description

The program consists of four basic parts. The first part of the program provides interaction with a user. The user is prompted for data concerning the geometry of the structure, the input pulse width and rise time, and data describing the loads at the ends of the lines.

The second part of the program calculates the inductance and capacitance coefficient matrices using the equations derived in chapter two. This part of the program takes more cpu time than the rest of the program combined due to the integrals (equations 2-40, 2-41, 2-42, and 2-43). This part of the program is not easily adaptable to microstrip transmission line systems with more than two signal conductors.

This is due to the increasing complexity and number of integrals that would have to be computed.

The third part of the program computes the eigenvalues and eigenvectors of the product of the inductance and capacitance coefficient matrices. Initial values for the modal transmission and reflection matrices are also computed here assuming that the system has not yet been excited.

The fourth part of the program consists of a loop which generates voltage steps into the system and propagates the voltage steps through the system. Each iteration through the loop represents an increment of time Δt given in figure 5. At the end of each loop new modal transmission and reflection matrices are calculated and the line load voltages are calculated from the modal load voltages and stored. None of the cross-coupled modes after the second reflection are propagated.

The third and fourth parts of the program are easily adaptable to transmission line systems with more than two signal conductors.

4.3 Linear Loads

Consider figure 6. The transmission lines are microstrip lines. The results in figures 7-9 all have the following parameters:

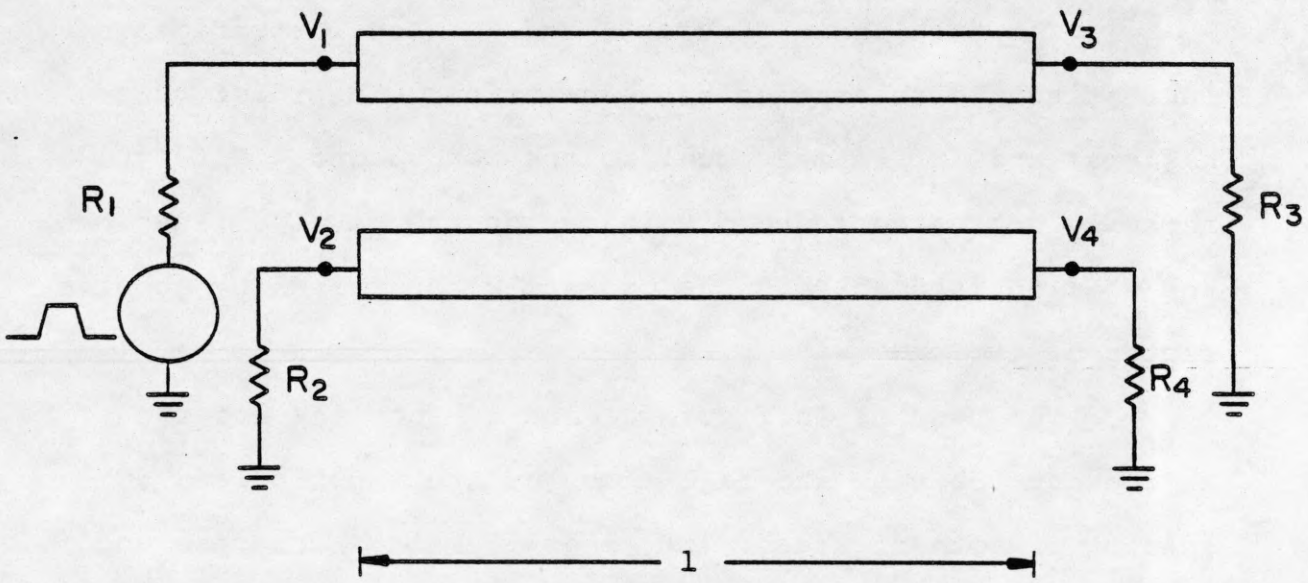

Figure 6 - Two-Line Transmission Line System

$R1 = 50\ \Omega$

$R2 = R3 = R4 = 100\ \Omega$

$\varepsilon_r = 5.0$

$l = .3$ m

$h = w = 10$ mils

pulse width = 6.0 ns.

The results in figures 7 and 8 show the effects of increasing the separation between strips. The input pulse has rise and fall times equal to one nanosecond. Note the markedly decreased induced voltages on the passive line when the spacing is doubled. The crosstalk has fallen by about a factor of two.

The results in figures 7 and 9 show the effects of shortening the rise and fall times of the input pulse. The spacing in both figures 7 and 9 is 10 mils. The rise and fall times of the input pulse in figure 7 is one nanosecond while the rise and fall times of the input pulse in figure 9 is .5 nanoseconds. The crosstalk increases substantially with decreasing rise and fall times showing the dependence of the crosstalk on the derivative of the input pulse.

In all cases the first-order reflections occurring at about 3.5 nanoseconds and about 10 nanoseconds have caused substantial shifts in the load voltages. Any later reflections are well damped. Thus, we can say that in these cases the simplification of not propagating any of the

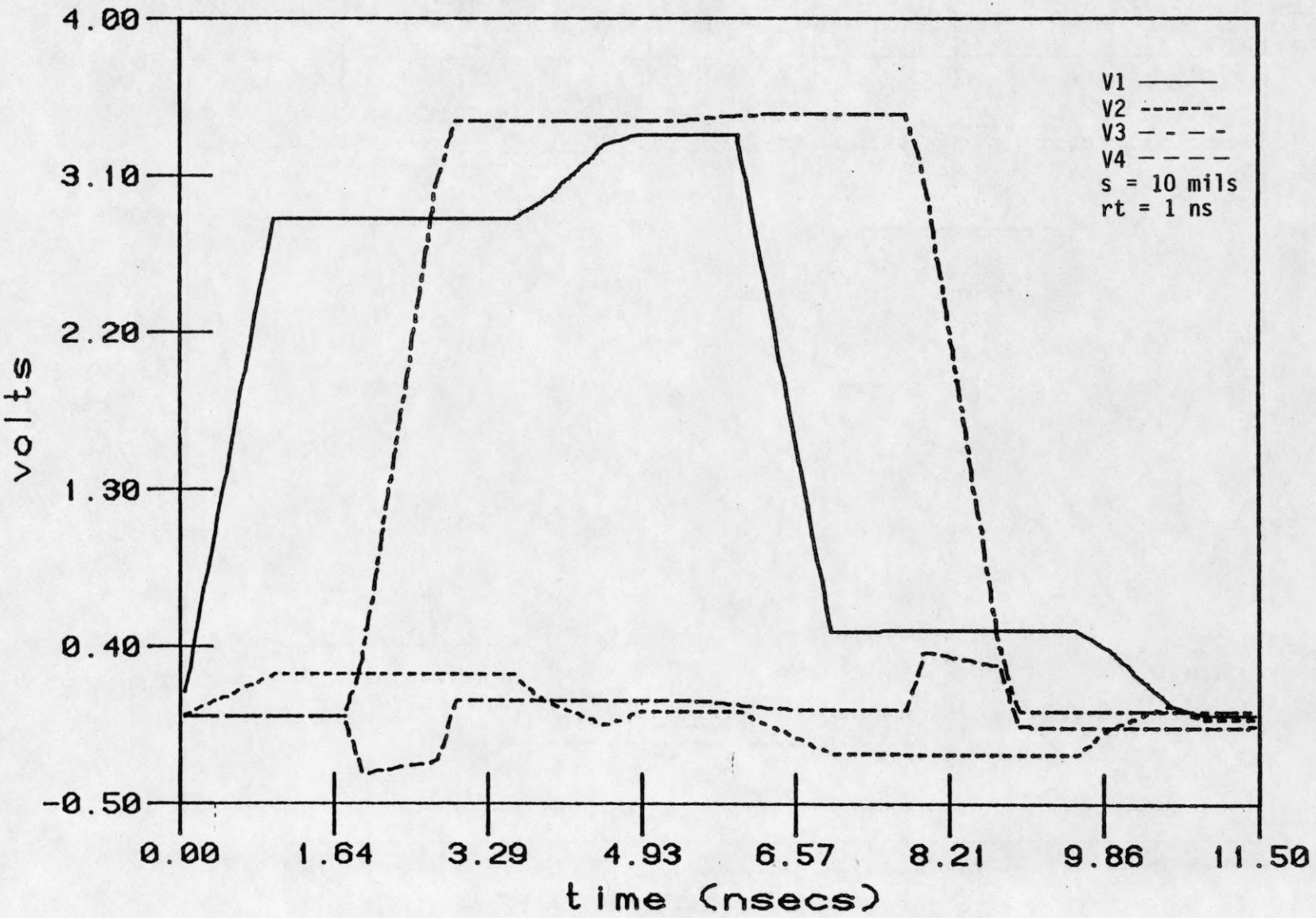

Figure 7 - Time Response of Two Line Transmission Line System

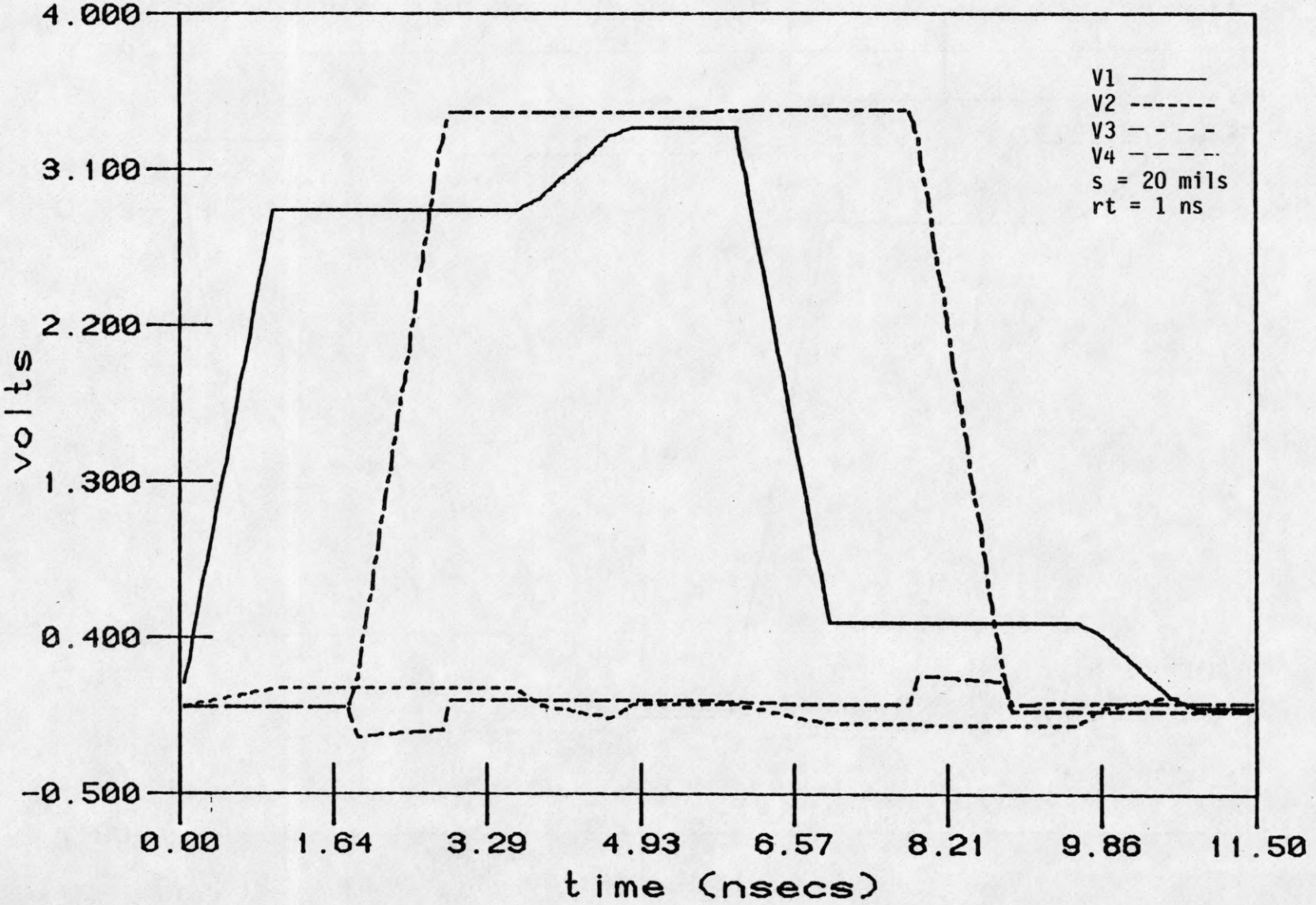

Figure 8 - Time Response of Two Line Transmission Line System With Increased Spacing

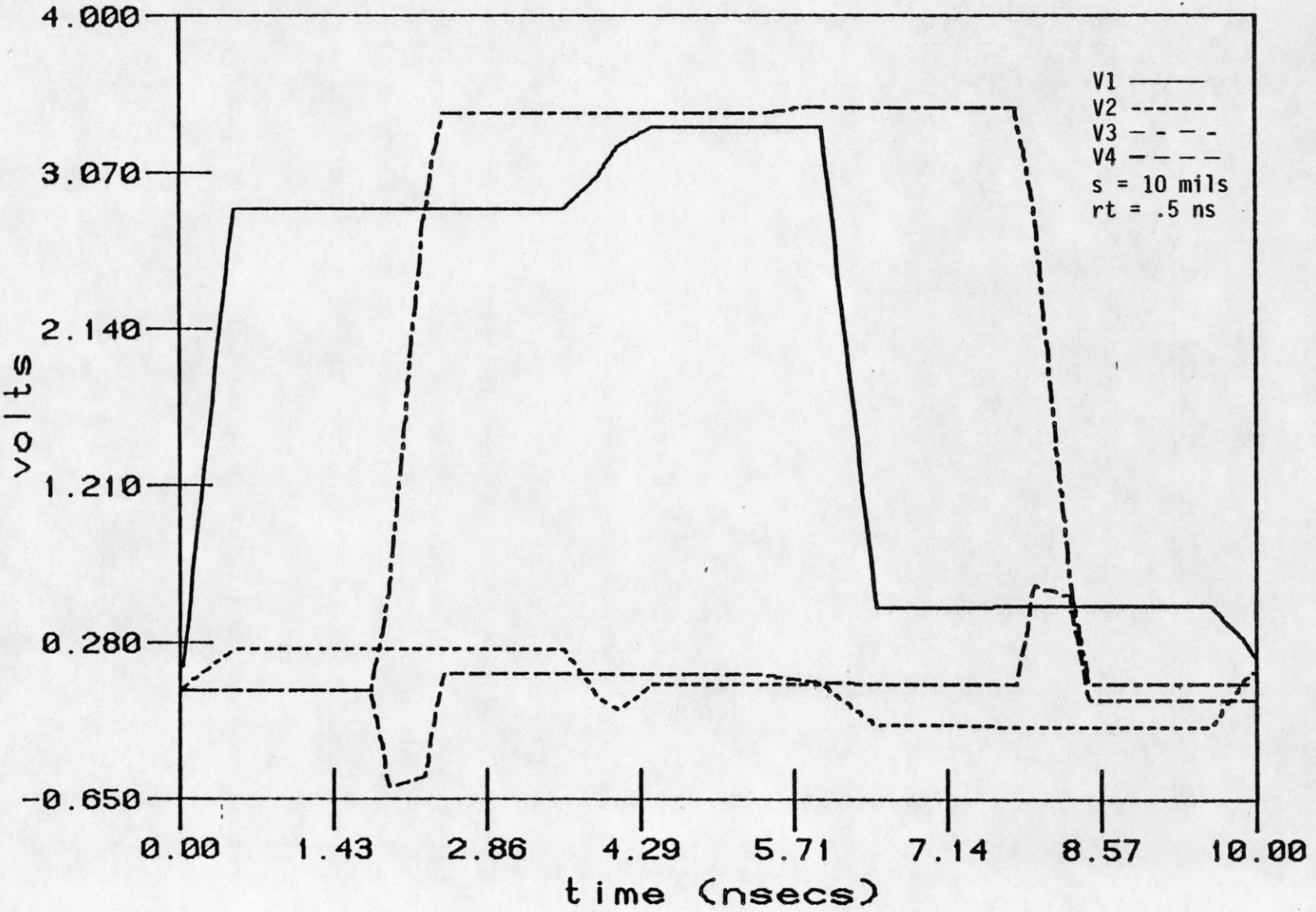

Figure 9 - Time Response of Two Line Transmission Line System With Decreased Rise Time

cross-coupled modes after the second reflection will not significantly alter the results.

4.4 Experimental and Theoretical Results

For figures 10 and 11 the following parameters were used:

R1 = 50 Ω

R2 = R3 = R4 = 88 Ω

εr = 5.0

l = .381 m

h = 21 mils

w = 20 mils

S = 5 mils

rise time = 1.0 nanoseconds

input voltage = .4 volts

The pulse width for the theoretical data shown in figure 10 is only 15 ns as compared with that for the experimental results which used an input pulse width of about 30 ns. This was done because of the limitation of the number of points that could be plotted by the plot routine being used.

Other than the difference in pulse widths, the theoretical data correspond very well with the experimental data.

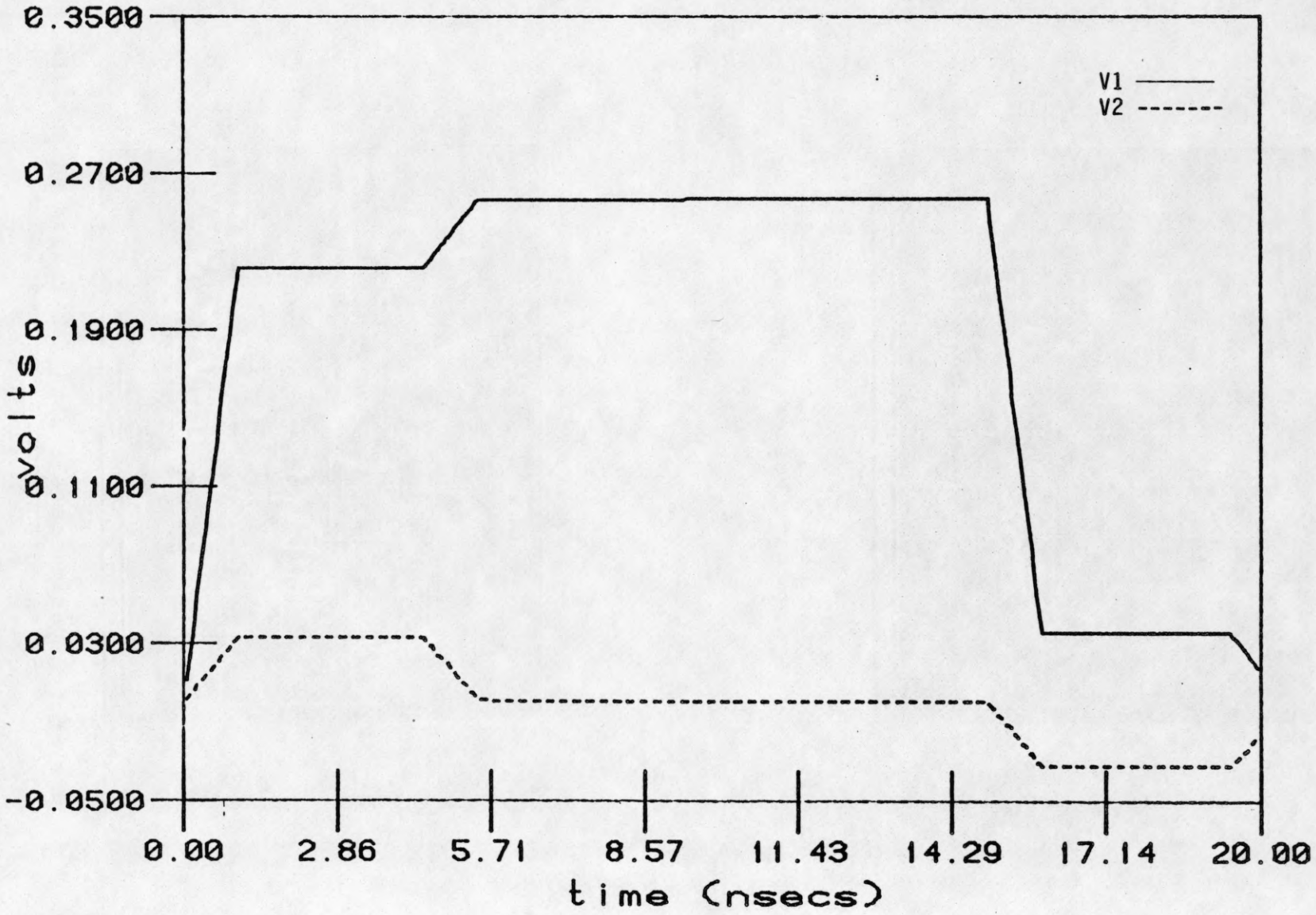

Figure 10 - Theoretical Results for Transmission Line System With Well Matched Loads

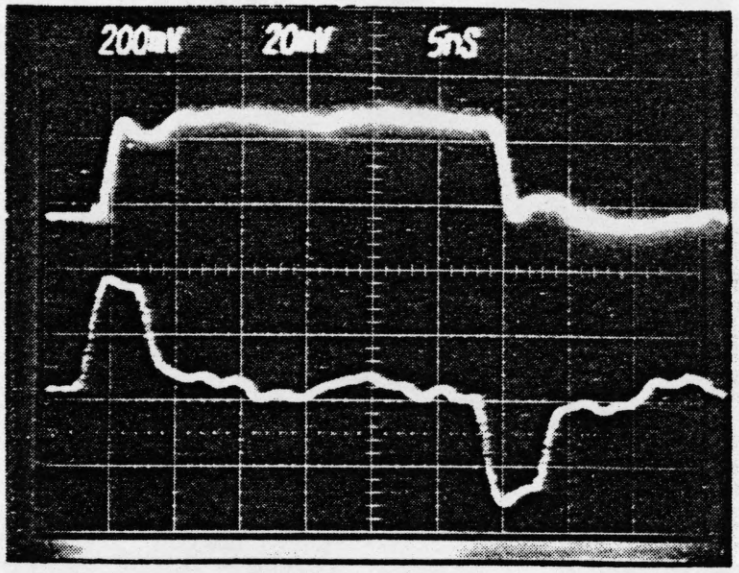

Figure 11 - Experimental Results for Transmission Line System With Well Matched Loads

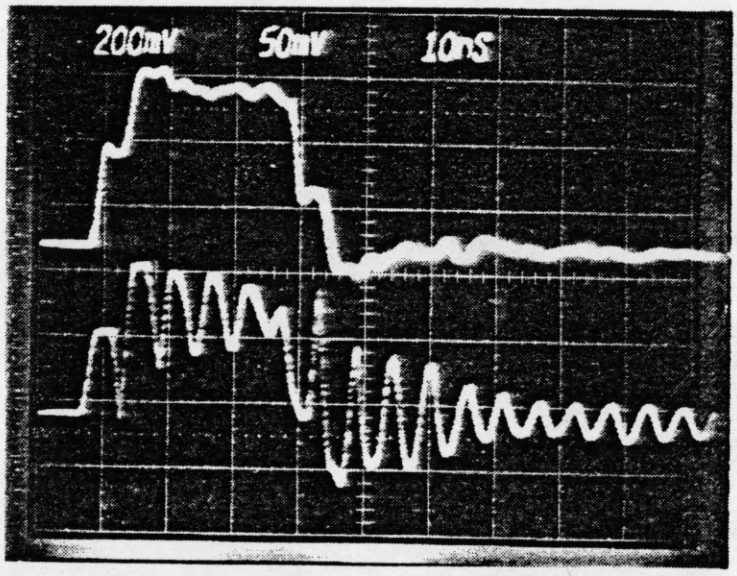

Figure 12 - Experimental Results for Transmission Line System With Poorly Matched Loads

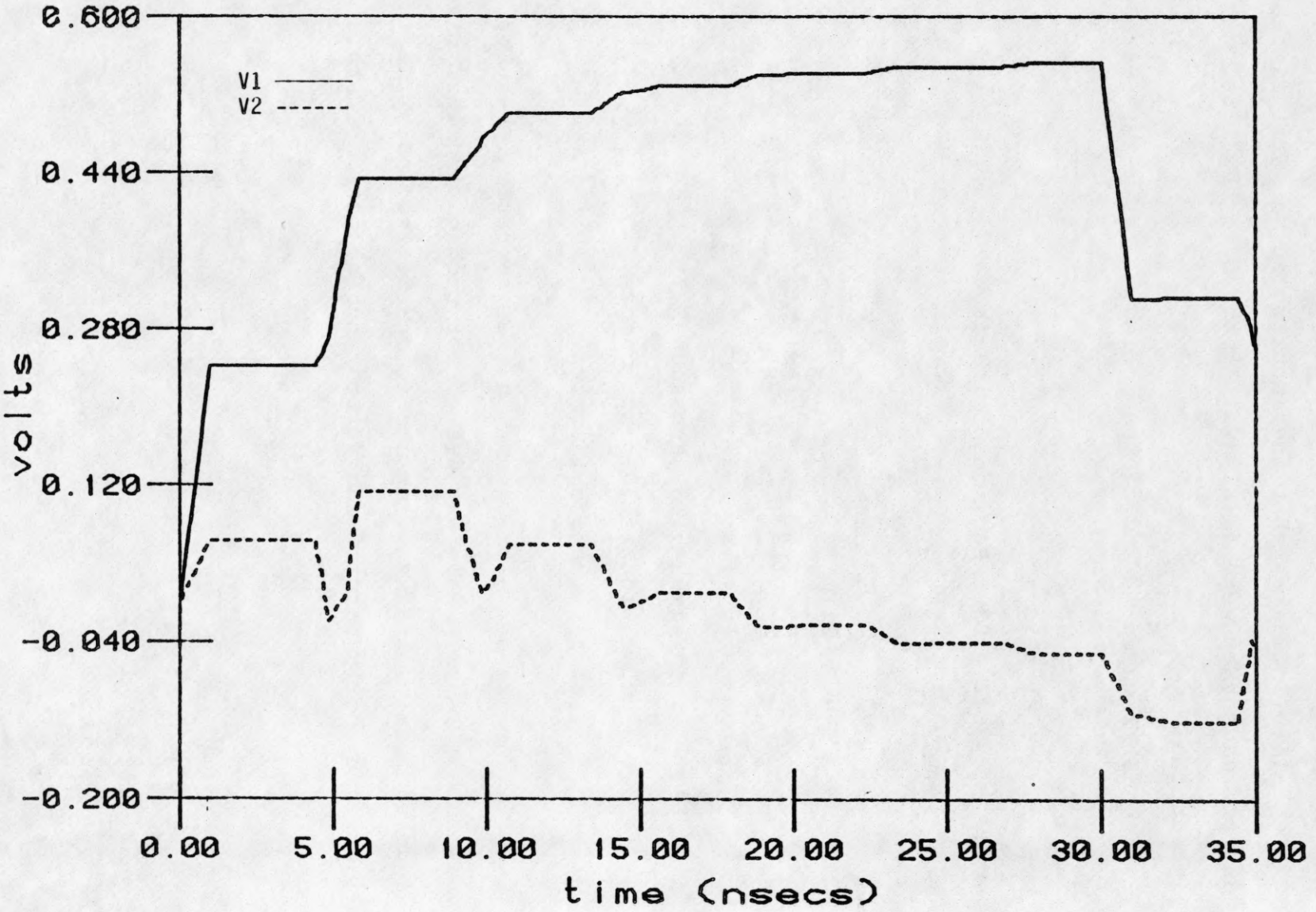

Figure 13 - Theoretical Results for Transmission Line System With Poorly Matched Loads

This indicates that the input pulse was well damped due to loads that were fairly well matched to the line impedances.

In figures 12 and 13 the following parameters were used:

R1 = 50 Ω

R2 = R3 = R4 = open circuit

ϵr = 5.0

l = .381 m

h = 21 mils

w = 20 mils

s = 10 mils

rise time = 1.0 nanoseconds

pulse width = 30 nanoseconds

input voltage = .4 volts.

Here we see a breakdown in the theoretical results past about 10 ns. This was due to not propagating the cross-coupled modal voltages after the second reflection. The loads are poorly matched and severe ringing occurs in this case.

5. CONCLUSIONS

In this report, we have studied the problem of calculating voltages at the ends of a three-conductor microstrip transmission line system. The problem of calculating the capacitance and inductance coefficient matrices was first solved. We first derived an integral equation relating voltage and charge by analyzing a simple transmission line model set up in the transverse direction of a microstrip structure. In a similar fashion, an integral equation relating magnetic flux and current was derived. The method of moments was used to solve for the unknown charges and currents. The resulting integrals were found to be very expensive to integrate so asymptotic methods were used to shorten the amount of computer time needed to solve these integrals. Once the currents and charges were solved for, then the capacitance and inductance coefficient matrices were easily solved for.

A method for finding the voltages at the loads of an N conductor transmission line system was presented. The telegrapher equations were combined to yield a second-order partial differential equation. A general solution to this equation was then substituted into the differential equation yielding an eigenvalue equation with the principal matrix being the product of the inductance and capacitance coefficient

matrices associated with the system. The resulting eigenvalues were one over the propagation velocities squared, and the eigenvectors were the modal amplitudes of the system. The result was that an N-conductor, transmission line system could be modeled as a single tube with N modes of propagation. The idea of modal transmission and reflection coefficient matrices was developed. The modal load voltages were then solved for by relating the incident and reflected modal voltages through the modal transmission and coefficient matrices.

In chapter four some results were presented which showed some of the difficulties of using time-domain methods for analyzing a transmission line system. The chief problem was the need for an expanding memory to keep track of cross-coupled modes produced when a single mode was incident upon a load. For loads fairly well matched to a transmission line system, an input pulse is damped quickly enough so that cross-coupled modes need not be propagated after the second reflection.

REFERENCES

1. T. Kitazawa and Y. Hayashi, "Propagation Characteristics of Striplines with Multilayered Anisotropic Media," IEEE Trans. Microwave Theory Tech., vol. MTT-31, pp. 429-433, June 1983.

2. J. Defalco, "Reflection and Crosstalk in Logic Circuit Interconnections," IEEE Spectrum, pp. 44-50, July 1970.

3. R. G. Saenz and E. M. Fulcher, "An Approach To Logic Circuit Noise Problems In Computer Design," Computer Design, pp. 84-91, April 1969.

4. A. Feller, H. R. Kaupp and J. J. Digiacomo, "Crosstalk And Reflections In High Speed Digital Systems," Proceedings - Full Joint Computer Conference, pp. 511-525, 1965.

5. C. F. Baum, T. K. Liu, F. M. Tesche, "On The Analysis of General Multiconductor Transmission-Line Networks," Interaction Note 350, November 1978.

6. A. Kjordjevic and T. K. Sarkar, "Analysis of Lossless Multiconductor Transmission Line Time Response," unpublished, July 1983.

7. R. F. Harrington, Field Computation By Moment Methods New York: Macmillan, 1968.

8. R. F. Harrington, Time Harmonic Electromagnetic Fields New York: McGraw-Hill, 1961.

9. I. S. Gradshteyn and I. M. Ryzhik, Table of Integrals Series And Products New York: Academic Press, 1965.

10. S. Frankel, Multiconductor Transmission Line Analysis Artech House, 1977.